International seminar on Nanoscience and Technology- conference proceedings. Oct- 2016
Volume 3, Special Issue - Available Online: http://ijrset.in/Volume3,Special-Issue-IV.php Pages: 17-23

ISSN 2394-739X
International Journal for Research in Science Engineering and Technology

EFFECT OF HOLMIUM DOPING ON THE STRUCTURAL AND OPTICAL PROPERTIES OF MAGNETITE NANOPOWDERS

[1] J. Sharmila Justus, [2] S. Dawn Dharma Roy, [3] A. Moses Ezhil Raj
[1]Department of Physics & Research Centre, Women's Christian College, Nagercoil – 629 001, Tamil Nadu, India.
[2]Department of Physics & Research Centre, Nesamony Memorial Christian College, Marthandam – 629165, Tamil Nadu, India.
[3]Department of Physics & Research Centre, Scott Christian College (Autonomous), Nagercoil – 629 003, Tamil Nadu, India.

ABSTRACT- Substantial amendment in structural and optical properties of magnetite nanoparticles could be done by incorporation of foreign cations, particularly facile for trivalent rare earth cations having different ionic radius. Adjoining holmium ions in native lattice was accomplished during solution synthesis approach using Iron (III) Chloride ($FeCl_3$) as starting precursor and Sodium Hydroxide (NaOH) as reducing agent without templates at low temperature. The growth and the controlled insertion of holmium ions in iron oxide particles were administered by regulating the pH of the solution using ammonium hydroxide. X-ray diffraction (XRD) analysis was performed to identify the structural modifications induced by the included dopant Ho^{3+} ions. Fourier transform infrared (FTIR) spectral studies identified the metal-oxide phase formation and the effect of dopant on modification of vibrational modes. Scanning electron microscope (SEM) was used to survey the changes in the morphology of the pure and doped Fe_3O_4 nanoparticles. Impregnated Ho content was measured by energy dispersive X-ray spectroscopy (EDS) analysis. Variations in the optical properties were identified from the recorded absorption spectral information in the wavelength range 200-2000 nm.

Keywords- [Sol-gel precipitation, nanopowder, XRD, FTIR, SEM, Optical]

1. INTRODUCTION

Rare-earth elements give trivalent cations, and they behave as very good dopants. Doping makes considerable changes in the properties of Fe_3O_4. Incorporation of foreign cations amends the particles' shape, induces change in optical properties, etc. The presence of foreign cations within the synthesis medium may also modify the product composition [1]. Highly monodispersed magnetite nanoparticles doped with Sm, Eu, Gd were prepared by thermal decomposition method and their magnetic properties were studied by Channa et al. [2]. Effect on magnetization was studied on Gd doped magnetite nanoparticles by Eun Sook Choi et al. [3]. Ho doped magnetite

nanoparticles were prepared by Maarten et al. [4] and their magnetic and magneto-optical properties were studied. Ho(III) shows characteristic luminescence. Chemical methods are useful in controlling the size, shape, composition, etc. We prepared Ho doped magnetite nanoparticles using modified precipitation method and the effect of doping on structural and optical properties were reported in this paper.

2. EXPERIMENTAL PROCEDURE

2.1. SYNTHESIS

Pure and holmium doped hematite nanoparticles were synthesized using ferric chloride (AR grade) and ethylene glycol as the starting materials. Initially, Iron (III) chloride was dissolved in a mixture of deionized water and ethylene glycol at room temperature for a concentration of 0.1M. The obtained solution was reduced using NaOH solution (0.1 M) to get a dark reddish brown clear solution. Resulted solution was kept in pH=11 by adding ammonia solution and stirred for 1h at 100ºC and then allowed to precipitate. The obtained precipitates were repeatedly washed with ethanol and distilled water and dried in air at 80ºC. This as-prepared sample was then annealed at 400ºC for 3 hrs. Thus pure magnetite nanopowders were obtained. For preparing holmium doped magnetite nanopowders, 1% of Holmium (III) nitrate was dissolved in the mixture of deionized water and ethylene glycol.

2.2. CHARACTERIZATION

X-ray powder diffraction (XRD) patterns of pure and doped α-Fe_2O_3 powder samples were recorded using a PANalytical-X'pert Pro X-ray diffractometer with Cu k_α radiation at room temperature (λ=1.5460 Å). Fourier transform infrared (FTIR) spectra were recorded on Rayleigh WQF-510 spectrophotometer in KBr pellet technique for the confirmation of metal oxide phase formation. Surface morphology of pure sample was characterized by using a JEOL JSM-6390 SEM operated at an accelerating voltage of 20 kV and that of doped sample was done by using JEOL JSM-7600F FEG-SEM operated at an accelerating voltage of 5 kV. The optical absorption spectra were taken on a Varian Cary 5000 UV–visible spectrometer.

3. RESULTS AND DISCUSSION

3.1. X-RAY DIFFRACTION ANALYSIS

The XRD pattern of the pure sample showed peaks at diffraction angles 2θ = 35.84° and 62.85° corresponding to the Miller indices (113) and (044) confirmed the formation of Fe_3O_4 nanoparticles with cubic inverse spinel structure [JCPDS Card No.: 96-101-1033]. The calculated d-value (2.50355 Å) is in agreement with the corresponding standard d-value of 2.50857 Å for magnetite [5]. Fe_3O_4 is a compound with Fe^{2+} and Fe^{3+} ions in an inverse spinel structure. The calculated lattice constant (a=8.343 Å) is slightly higher than the standard value (a=8.32 Å) that may be attributed to the small size of the particles. The crystallite size of the particles estimated using Debye-Scherrer formula was found to be 6 nm. The other related structural parameters were also estimated and are listed in Table 1.

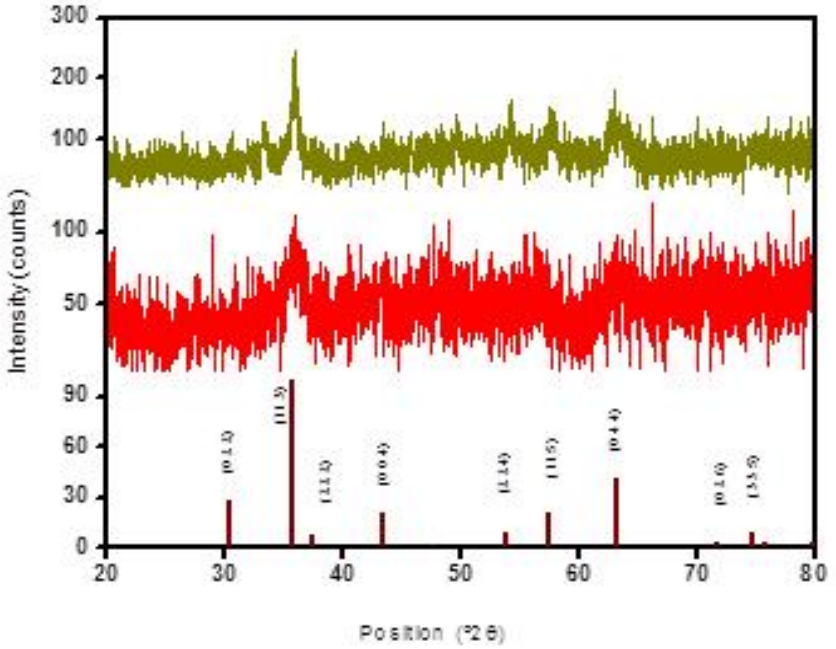

Figure 1 XRD Patter of the prepared magnetite nanopowders:(a) pure (b) Ho doped

Sample Details	**Lattice Parameter (Å)**	**Unit cell Volume (Å)^3**	**Density (g/cm^3)**	**Crystallite Size (nm)**	**Dislocation density x10^{15} (lines/m^2)**	**Microstrain**
Pure	8.343	580.712	5.295	6	28.036	0.0264
Ho doped	8.3208	576.086	5.3375	17	3.5647	0.0067
Standard value	8.320	575.93	5.34	-	-	-

Table 1 Structural parameters of the prepared Fe_3O_4 nanoparticles

The XRD pattern of the doped sample showed six peaks of which three peaks including the most intense peak match with the JCPDS Card No.: 96-101-1033. The other peaks match with JCPDS file no. 01-079-0007 of the hematite phase. Hence, the doped sample is in mixed phase containing octahedrally and tetrahedrally coordinated Fe^{3+} ions and otahedrally coordinated Fe^{2+} ions. The structural parameters were calculated for the cubic inverse spinel structure and are also listed in the Table 1.The incorporated dopant ions modify the cell edge and cause a change in unit cell volume and density. The crystallite size of the doped sample is greater than that of the pure sample which is a contradiction and this is due to formation of mixed phase.

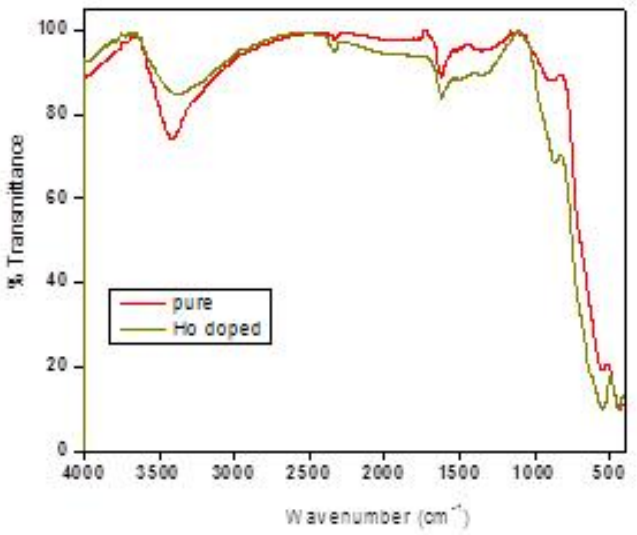

Figure 2- FTIR Spectra The Magnetite nanopowders (a) Pure (b) Ho doped

3.2. FTIR SPECTROSCOPY

FTIR spectroscopy helps to identify the various polymorphs of iron oxide. Fe_3O_4 contains tetrahedrally and octahedrally co-ordinated Fe and O ions and the bulk Fe_3O_4 has two absorption bands at 375 and 570 cm^{-1} [6]. The FTIR curve of the pure sample shows broad bands at 432 and 553 cm^{-1} that can be assigned to the bending and stretching vibration of Fe-O bond in the tetrahedral and octahedral sites of cubic inverse spinel structure confirming the product as magnetite [7]. The bands found at around 3389 cm^{-1} indicate the stretching modes of H_2O molecules or OH groups and that at around 1619 cm^{-1} is assigned to the bending vibrations of H_2O on the surface of the particles [8, 9]. The doped sample has two bands at 454 and 553 cm^{-1}. The band found at 432 cm^{-1} disappeared and the band now seen at 454 cm^{-1} is ascribed to the Fe-O bending vibration mode of α-Fe_2O_3 [10]. Therefore, the presence of α-Fe_2O_3 is confirmed which was already identified through XRD.

3.3. SEM ANALYSIS

Fig. 3(a) shows the SEM image of the pure Fe_3O_4 nanoparticles. The particles are agglomerated and are not having regular shape. Its size distribution is also not uniform. The average size of the agglomers is 0.4 µm. Their elemental composition is observed from the recorded EDAX spectra shown in the inset of the figure. It reveals the presence of O and Fe elements and no signals of other elements present indicate that the products are pure. The SEM image of the doped sample shows that the particles are spherical in shape. But, still the particles are agglomerated. The average size of the agglomers is 0.25 µm. The EDAX spectrum of the doped sample shows some additional peaks corresponding to the element Ho. The noted EDAX spectra spectacles the increment of Fe content (74%) and suppression of O content. α-Fe_2O_3 is a metal rich compound and rise in Fe content confirms the presence of hematite also in the doped sample. Thus, the doped sample is a composition of magnetite and hematite.

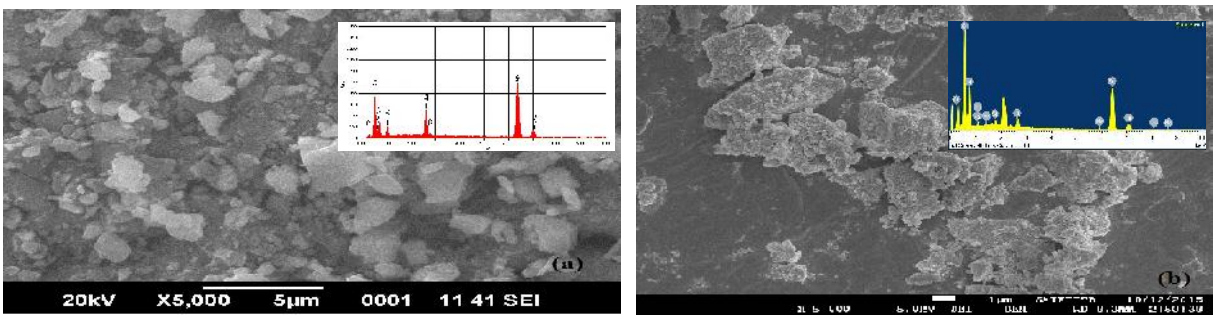

Figure 3- SEM images of the magnetite nanopowders: (a) pure (b) Ho doped

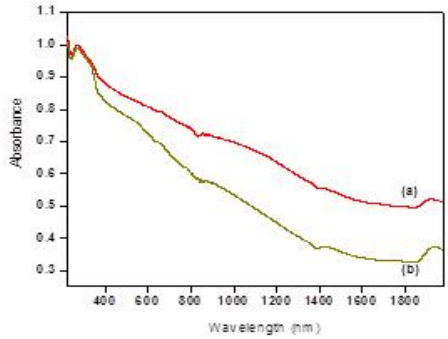

Figure 4- Vis absorption Spectra of the magnetite nanopowders (a) pure (b) Ho doped

3.4. UV-Vis spectroscopy

Fig. 4 shows the absorption spectra of the pure and the Ho doped sample at room temperature. The absorption peak noticed at 270 nm can be assigned to the metal to ligand charge transfer interactions. The peak observed at 335 nm is due to the charge transfer between the cations present in the octahedral and tetrahedral sites of Fe_3O_4. Fe_3O_4 shows both direct and indirect band gaps [11]. Both the energy band gaps were calculated using the Tauc equation, $(\alpha h\nu)^{1/n} = B\ (h\nu - E_g)$, where $h\nu$ is the incident photon energy, α is the absorption coefficient, B is a material-dependent constant and E_g is the optical band gap. The value of n depends on the nature of transition. For direct allowed transition, n=1/2 and for indirect allowed transition n=2. Tauc plots drawn by taking $(\alpha h\nu)^{1/n}$ along the y-axis and $h\nu$ along the x-axis is shown in Fig. 5 and 6.

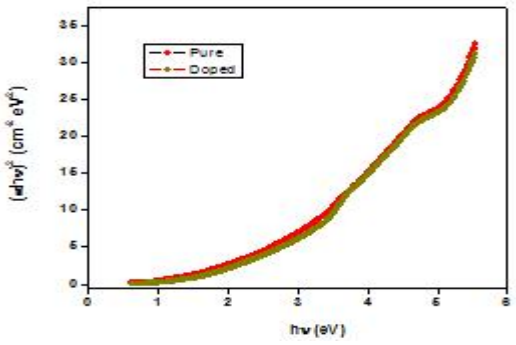

Figure 5-Variation of $(ahv)^2$ Vs. Photon evergy

The energy band gap values of the samples were calculated by extrapolating the linear portion of the curve. The literature values and the calculated values of the direct and indirect band gap values are listed in table 2. The direct band gap values are found to be greater than the indirect band gap. Both the direct and indirect band gap values for the Ho doped sample are found to be greater than the pure sample. Usually, as the size increases the energy gap must increase. But, in our work the band gap also increases and this may be due to the presence of mixed phase. The calculated values are found to be less than the literature values. However, it is in the range of semiconductor energy band gap (0-3 eV) [12]. Thus, magnetite is a semiconductor.

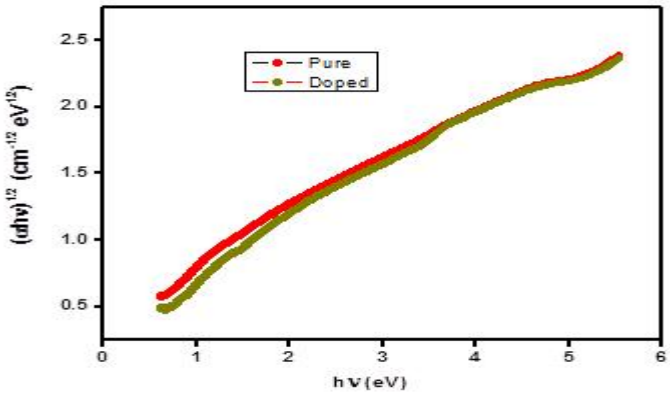

Figure 6- Variation of $(ahv)^{1/2}$ vs photon energy

Nature of transition	Literature value [11]	Pure	Doped
Direct	2.9	2.45	2.50
Indirect	1.9	0.51	0.60

Table 2 Band gap values of the magnetite nanopowders in eV

CONCLUSION

Pure and holmium doped magnetite nanoparticles were prepared by controlling the pH value of the starting precursor solution. Incorporation of the dopant Ho ion into the lattice was identified from the XRD studies and confirmed through FT-Raman and EDAX studies. Replacement of Fe ions by Ho ions amended the product composition, the lattice constant. Surface morphological studies confirmed the induced amendments in shape, size and distribution of the crystallites due to the dopant ion. Both the direct and indirect band gap increases on replacing the native Fe ions with Ho ions.

ACKNOWLEDGEMENTS

We thank Sophisticated Test and Instrumentation Centre, Cochin University, Kerala for their assistance in using SEM, FTIR and UV-vis facilities. We are also grateful to Sophisticated Analytical

Instrument Facility, IIT Bombay, Mumbai for providing FEG-SEM facility.

REFERENCES

[1] Francesca Stefania Freyria, Gabriele Barrera, Paola Tiberto Elena Belluso, Davide Levy, Guido Saracco, Paola Allia, Edoardo Garrone, Barbara Bonelli, Journal of Solid State Chemistry 201 (2013) 302
[2] Channa R. De Silva, Steve Smith, Inbo Shim, Jeffrey Pyun, Timothy Gutu, Jun Jiao, Zhiping Zheng, Journal of American Chemical Society 131 (2009) 6336
[3] Eun Sook Choi, Wenlong Xu, Myun Ju Baek, Ja Youn Park, Joo Hyun Kim, Yongmin Chang, Tae Jeong Kim, Gang Ho Lee, AIP Advances 3 (2013) 072101
[4] Maarten Bloemen, Stefaan Vandendriessche, Vincent Goovaerts, Ward Brullot, Maarten Vanbel, Sophie Carron, Nick Geukens, Tatjana Parac-Vogt, Thierry Verbiest, Materials 7 (2014) 1155
[5] Hironori Iida, Kosuke Takayanagi, Takuya Nakanishi and Tetsuya Osaka, Journal of Colloid and Interface Science 314 (2007) 274
[6] J. L. Zhang, R. S. Srivastava and R. D. K. Misra, Langmuir 23 (2007) 6342
[7] Lingyun Chen, Zhen Lin, Chenglan Zhao, Yiyang Zheng, Yang Zhou and Hui Peng, Journal of Alloys and Compounds 509 (2011) L1
[8] F. Dang, N. Enomoto, J. Hojo and K. Enpuku, Ultrasound Sonochemistry 16 (2009) 649
[9] B. Stuart, in Infrared Spectroscopy: Fundamentals and Applications, John Wiley & Sons, Ltd., New York (2004)
[10] F. Wang, X.F. Qin, Y.F. Meng, Z.L. Guo, L.X. Yang, Y.F. Ming, Materials Science in Semiconductor Processing 16 (2013) 802
[11] H. El Ghandoor, H. M. Zidan, Mostafa M.H. Khalil, M.I.M. Ismail, International Journal of Electrochemical Science 7 (2012) 5734
[12] Sachnin A. Kulkarni, P. S. Sawadh, Prakash K. Palei, Kiran K. Kokate, Ceramics International 40 (2014) 1945